Journal of the Meteorological Society of Japan, Vol. 77, No. 5, pp. 1007–1021, 1999

Estimate of the Cloud and Aerosol Effects on the Surface Radiative Flux Based on the Measurements and the Transfer Model Calculations Part I: Shortwave Forcing at Tateno, Japan

By Yukari N. Takayabu

National Institute for Environmental Studies, Tsukuba, Japan

T. Ueno

Aerological Observatory, Japan Meteorological Agency, Tsukuba, Japan

T. Nakajima

Center for the Climate System Research, University of Tokyo, Komaba, Japan

I. Matsui

National Institute for Environmental Studies, Tsukuba, Japan

Y. Tsushima

Frontier Research System for Global Change Prediction, Tokyo, Japan

K. Aoki

Hokkaido University, Sapporo, Japan

N. Sugimoto

National Institute for Environmental Studies, Tsukuba, Japan

and

I. Uno

University of Kyusyu, Fukuoka, Japan

(Manuscript received 22 January 1998, in revised form 30 June 1999)

Abstract

In order to estimate the annual surface shortwave forcing by clouds+aerosols and aerosols, the shortwave flux from pyrheliometer and pyranometer measurements, atmospheric profiles from the radiosonde measurements, and aerosol optical properties retrieved from sky radiometer measurements were integrated with high-accuracy transfer model calculations.

Corresponding author: Yukari N. Takayabu, National Institute for Environmental Studies, 16-2 Onogawa, Tsukuba, 305-0053, Japan. E-mail: yukari@nies.go.jp

Clear-sky flux was defined from transfer calculations for a pure Rayleigh-scattering atmosphere, with measured temperature and humidity profiles by radiosonde observations. Monthly variation of the clear-sky flux due to the temperature and water vapor variation was 10–30 $W m^{-2}$. Cloud+aerosol forcing was defined by the difference between the observed flux and the clear-sky flux (positive downward). The annual mean values of the cloud+aerosol surface shortwave forcing was estimated as -81 $W m^{-2}$, which corresponds to about 24 % of the insolation. The aerosol-sky flux is defined with the transfer calculation using the aerosol optical depth retrieved from the sky radiometer measurements. Aerosol forcing was obtained from the differences between the clear-sky flux and the aerosol-sky flux. The mean direct aerosol forcing for 1996, except for March and April, was estimated as -18 $W m^{-2}$, about 6 % of the insolation.

We also performed a sensitivity study of the aerosol-sky flux by varying the weight fraction of soot in aerosols. Among the selected soot fraction, the best estimates were obtained as 10 % for January, February and July, 20 % for October through December, 5 % for May, June and August, and 0 % for September. These values are close to the measured seasonal variations of soot fraction in previous studies.

Surface flux calculation with the retrieved aerosol size distributions performed no better than those with the LOWTRAN 7 urban model size distribution, especially in the summer months when the water vapor column amount was large. The necessity of further examination of retrieval methods of aerosol optical properties, using sky radiometer measurements, was suggested.

1. Introduction

There have been disputes over the discrepancy by 10–30 $W m^{-2}$ between the observed, and the model calculated atmospheric absorptance (Cess *et al.*, 1995; Ramanathan *et al.*, 1995; Pilewskie and Valero, 1995; Wild *et al.*, 1995; Arking, 1996; Stephens, 1996). These disputes are based on the estimates of the cloud radiative forcing at the top of the atmosphere and at the surface. The cloud radiative forcing is defined by the difference between the all-sky flux, and the clear-sky flux at a specified level. However, there are inherent difficulties to define the clear-sky flux from the observation alone, due to the variations of the water vapor and aerosol loadings on the clear sky. The side effects of finite clouds could result in the erroneous flux convergence estimates (Hayasaka *et al.*, 1995). As for the model calculations, on the other hand, it is difficult to obtain the all-sky flux, because the plane-parallel assumption is not valid for the real atmosphere with inhomogeneous clouds. Also, cloud data large enough to be utilized for the model calculation are not available.

The importance of the aerosol radiative effects in the climate has been emphasized in the context of global warming (Charlson *et al.*, 1992; Kiehl and Briegleb, 1993). Sensitivity of the aerosol radiative effects to the aerosol chemical composition and size distribution was also examined (Pilinis *et al.*, 1995; Haywood and Shine, 1995). Many of these estimates were based on the specified aerosol loading, but observational estimates of aerosol radiative forcing have been scarcely done.

More recently, some studies reevaluated the surface clear-sky flux utilizing more precise surface observations (Chou and Zhao, 1997; Conant *et al.*, 1997). These studies proposed statistical methods to estimate the clear-sky flux utilizing the surface radiation measurements with high temporal resolutions. Conant *et al.* (1997) proposed the peak frequency density method to estimate the clear-sky flux utilizing radiation measurements of the CEPEX (Central Equatorial Pacific Experiment) with a high temporal resolution (10-sec). This method is unique because the precision of the clear-sky measurements (or its variation depending on the atmospheric conditions) is obtained statistically with the transmittance estimate. There are some limitations, however, such as the valid solar zenith angle is limited to less than 45°, and its application to the region with larger cloudiness is probably not adequate. Chou and Zhao (1997) proposed a method to utilize the 1-min measurements of direct and diffuse downward solar flux to obtain the clear-sky surface flux, and applied it to the TOGA COARE (Tropical Ocean and Global Atmosphere Coupled Ocean-Atmosphere Response Experiment) observational data. They validated the radiative model calculation of the clear-sky flux, with specified aerosol optical parameters, and utilized it to estimate the clear-sky flux and the cloud radiative forcing. Their method was shown to be valid for the situation over the open ocean. However, over the land where large variations of the aerosol parameters are expected, more precise treatments of aerosols are indispensable for the clear-sky flux calculations, for the estimates of the aerosol effects, and for their validations. Also, in previous studies, the analysis periods were limited to one to several months.

At Tateno, the Aerological Observatory of the Japan Meteorological Agency, the National Institute for the Environmental Studies, and the Meteorological Research Institute are located close to each other. This situation yielded quality-controlled long-term data from various observational platforms: direct, diffuse and reflected solar flux observed with a system which meets the standard of the Baseline Surface Radiation Network (BSRN); 12-hourly radiosonde upper-air soundings; and, sky radiometer measurements from which aerosol optical properties can be retrieved.

The objective of this study is to estimate the cloud

and/or aerosol radiative forcing with a high accuracy for one year of 1996, making use of high quality and unique data set.

It was shown in the previous studies, that even with the high temporal resolution data, purely observational estimates of the clear-sky flux cannot avoid the uncertainties resulting from the presense of clouds, finite cloud effects, water vapor variations, and aerosol loading. On the other hand, these studies indicated that radiative transfer calculations with high accuracy methods are quite promising (Chou and Zhao, 1997; Conant *et al.*, 1997).

In this study we utilize the state-of-the-art radiative transfer model with the observed atmospheric profiles for the clear-sky flux estimates. An advantage of this method is that the clear-sky flux can be defined as the pure Rayleigh-scattering atmosphere without clouds or aerosols. Secondly, clear-sky flux can be calculated even for the cloudy days utilizing the observed atmospheric profiles of humidity and air temperature. Although the radiative forcing is defined by the difference between the clear-sky flux and the all-sky flux, these values can not be observed simultaneously. Our method is preferable for obtaining the cloud (and aerosol) radiative forcing in an accurate sense. As for the all-sky flux, observed flux values are utilized, since model calculations of all-sky flux with cloud data are not free from the problematic treatments of the inhomogeneous or broken clouds.

The primary advantage of this study is the availability of the observed aerosol optical data. Observed clear-sky flux is, in an exact sense, an aerosol-laden-sky flux. First, we can obtain the aerosol forcing from the difference between the observed clear-sky flux, and the calculated clear-sky flux. Second, we can validate the model calculation by comparing the flux calculated with the observed aerosol data and the observed clear-sky flux. It can be expected that the accuracy of the calculated true clear-sky flux values of the Rayleigh-scattering atmosphere is higher than that of the aerosol-laden-atmosphere.

The largest uncertainty in the aerosol-sky flux resides in the complex refractive index of the aerosols. In order to estimate the aerosol forcing at the surface accurately, it is indispensable to determine the soot fraction properly (Nakajima *et al.*, 1996). Here, sensitivity studies were also performed by varying the weight fraction of soot in aerosols used in the transfer model calculations. Finally, the annual mean values for the cloud and/or aerosol surface shortwave forcings were estimated with the most adequate soot weight fraction for each month.

2. Methods for the radiative forcing estimate

In order to exclude the influence of the aerosol forcing in the clear-sky flux, we define the clear-sky flux obtained from the transfer model calculation with the Rayleigh-scattering atmosphere.

Then, the cloud+aerosol forcing (CAF), the aerosol forcing (AF), and the estimated error for the aerosol-sky flux (Aerror) are defined as:

- CAF = Fall(obs) - Fclear(calc), (1)
- AF = Faero(calc) - Fclear(calc), (2)
- Aerror = Faero(obs) - Faero(calc), (3)

where Fall(obs) stands for the observed all-sky net flux (with clouds and aerosols), and Fclear(calc) is the calculated clear-sky flux. Faero(calc) and Faero(obs) are calculated and observed flux, respectively, for the aerosol-laden atmosphere without clouds (hereafter referred to as the aerosol-sky). Signs of flux are defined positive downward. Descriptions about the data for observed values are found in the following section.

Flux calculations were separately performed for the clear-sky and for the aerosol-sky. Clear-sky calculations were done every 15 minutes utilizing the interpolated water vapor and temperature profiles with varying solar zenith angles. The vertical profiles of other atmospheric gases were adopted from the LOWTRAN 7 model profiles of the mid-latitude summer for the months from April to September and that of the mid-latitude winter for other months. For every minute when the sky radiometer measurement was available, the aerosol-sky flux was also calculated utilizing the aerosol optical thickness retrieved from the sky radiometer data with the same atmospheric profiles as that used for the clear-sky flux calculation.

The sky radiometer measurements were carried out in the clear-sky situation. In order to further screen out the cloud effects, we introduced a rms threshold with the observed diffuse flux. When the standard deviation of the observed diffuse flux in the neighboring 30 minutes exceeds 12 % of the total insolation, we decided that there are cloud contaminations, and excluded the data from the aerosol-sky flux calculations.

For the transfer calculation, the version FSTAR5b of the general package R-star in the System for Transfer of Atmospheric Radiation (STAR) series, which was developed by the University of Tokyo, and Munich University, was utilized. The R-star package is based on the algorithms of Nakajima and Tanaka (1983, 1986, 1988), and a LOWTRAN 7 gas absorption model (Kneizys *et al.*, 1986).

Following settings were selected for our calculations:

- For scattering calculations, four-stream TMS (Truncated Multiple+Single Scattering) method was selected.
- For subchannel calculations, k-distribution method was utilized.

- Flux were calculated at 29 levels: 1, 2, 3, 4, 5, 6, 7, 8, 9, 10, 11, 12, 13, 14, 15, 16, 17, 18, 19, 20, 22, 24, 26, 28, 30, 32, 35, 40, 45, and 50 km.
- Integrations were done for the wavelength range of 0.3–3.0 μm, divided in 200 subranges.
- Observed temperature and relative humidity were interpolated to 50 model levels with the Spline fitting for the model input.
- Monthly-mean ground reflectivity obtained from the observed showrtwave flux was utilized for the upward-flux calculations.
- Retrieved aerosol optical depth at 0.5 μm were utilized. As for the aerosol size distribution, transfer calculations were done with the retrieved size distribution as well as with the LOWTRAN 7 model size distribution of the urban/rural aerosols.
- Sensitivities to the soot mass fraction in aerosols were examined.
- In order to avoid the dependence of the retrieved optical depth on the assumed optical features, the optical depth was also retrieved with the sunphotometry method; the sensitivity tests were performed with these values.

3. Data and analysis period

Following data during the period of 1 January to 31 December in 1996 were used for the analysis and calculations,

- One-minute average archives of direct, diffuse and reflective solar flux data were obtained from the pyrheliometer (Eppley, NIP) measurements and the pyranometer (EKO MS801F, KIPP CM11) measurements for wavelengths of 0.3–3.0 μm at the Tateno Aerological Observatory. This flux measurement system at Tateno meets the standard of the Baseline Surface Radiation Network.
- Twice daily vertical profiles of the relative humidity and air temperature were obtained from the radiosonde soundings at the Tateno Aerological Observatory.
- Aerosol optical thickness and size distribution were retrieved every 15 minutes for clear-sky situation from the sky radiometer measurements at the National Institute for Environmental Studies and at the Meteorological Research Institute. Note that data acquisition by the sky radiometer was limited to the periods of 1 January–2 February, 1 May–11 July, and 31 July–31 December in 1996. Therefore, the data for March and April 1996 were missing, and those for February and July were incomplete.
- Twice daily wind profiles obtained from the radiosonde soundings at the Tateno Aerological Observatory were also utilized supplementarily for the interpretation of the sensitivity experiments to the weight fraction of the soot in aerosols.

4. Clear-sky flux calculations

An example of the calculated clear-atmosphere flux (blue dots), and the 1-minute averaged net (downward-upward) shortwave flux observed at the surface (red dots), for June 1996 is shown in Fig. 1. It is confirmed that calculated clear-sky fluxes almost correspond to the upper bound of the observed fluxes, except for some anomalously large observed values. These anomalous values are thought to result from the side effects of the finite clouds (Hayasaka *et al.*, 1995). It is also found that the clear sky flux has a certain variation of almost 80 W m^{-2} for small solar zenith angles, which is indicated from the width of the band of blue dots. This variation is attributable primarily to the variation of the water vapor contents in the atmosphere.

A close examination of the figure reveals that some numbers of relatively continuous distributions of red dots (observed net flux) are embedded in the scatter. While the atmosphere is in nearly plane-parallel conditions, the observed fluxes are expected to exhibit such continuous distributions in this plot. Some upper-bound flux methods to obtain the clear-sky flux (*e.g.*, Ramanathan *et al.*, 1995) use such smooth distributions as the clear-sky values. However, there are obvious discrepancies between the calculated clear-sky flux values and these continuous distributions. These discrepancies are attributable to the aerosols and/or thin clouds.

The above results infer that there are at least two inherent difficulties in determining the clear-sky flux purely from the observations: (1) the atmospheric profiles vary considerably due to water vapor loading, and (2) there is significant aerosol forcing which also varies largely with the variation of aerosol amounts.

In order to grasp the variation of the water vapor loading, the change in daily-averaged amount of the column water vapor at Tateno in 1996 is shown in Fig. 2. The column water vapor amount stays relatively low from January through April. It increases quite abruptly from the latter half of May through June. From the latter half of June through August, a large column water vapor around 45 kg m^{-2} is maintained. It gradually decreases from September through November, and comes back to the wintertime low values in December. Daily variations of the column water vapor amount is about 20 kg m^{-2} for

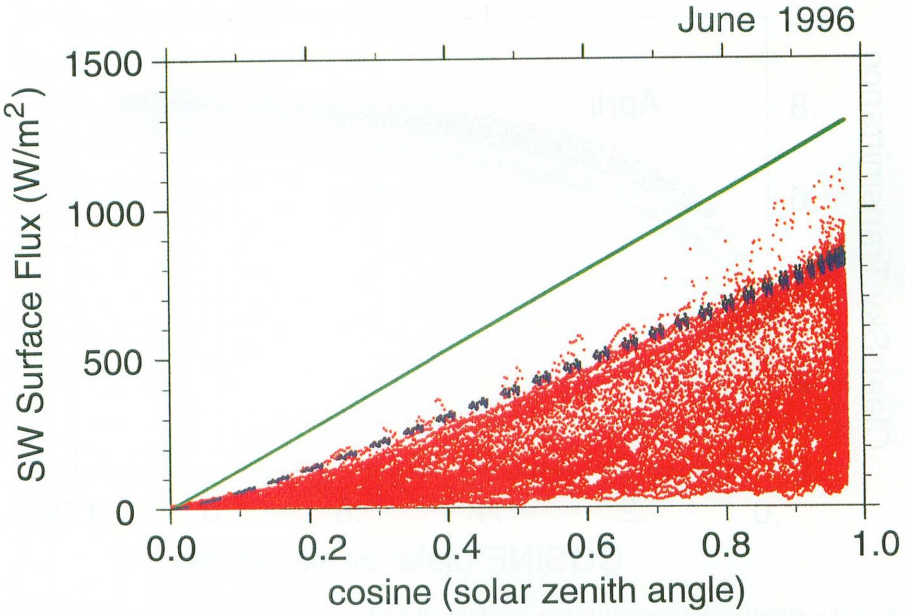

Fig. 1. Observed net surface solar flux (red dots) and the calculated clear-sky surface shortwave flux (blue dots) plotted against the cosine of the solar zenith angle. Thick green straight line depicts the insolation at the top of the atmosphere. The data for one month of June 1996 are shown.

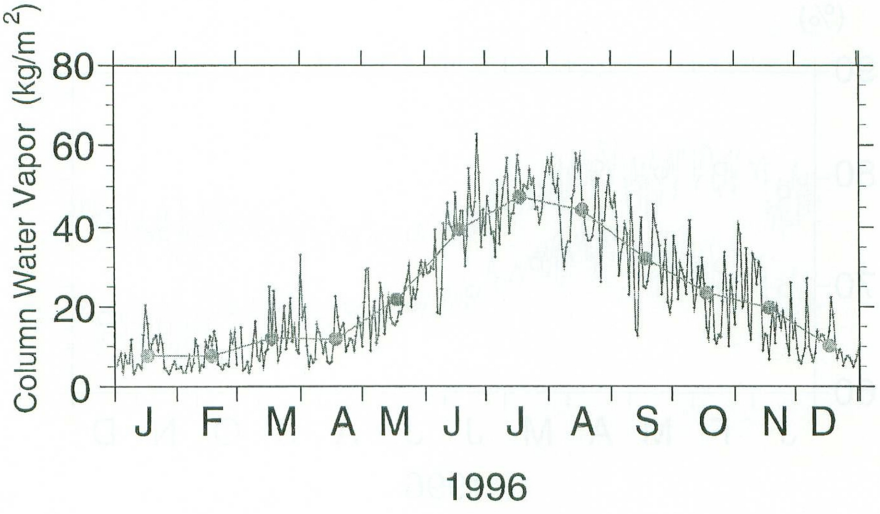

Fig. 2. Change in daily-mean amount of the column water vapor in kg m^{-2} for 1996. The value was obtained by integration of the water-vapor concentrations from surface to 100 hPa using the Tateno radiosonde soundings. Larger dots indicate the monthly mean values.

warmer seasons, and 10–15 kg m^{-2} for cooler seasons.

Monthly-mean amounts of the column water vapor for April and July are about 12.5 kg m^{-2}, and about 47.5 kg m^{-2}, respectively. Figure 3 compares the calculated clear-sky transmittance plotted against the cosine of the solar zenith angle for April and for July. The transmittance is evaluated by the ratio of the surface downward flux to the TOA (top of the atmosphere) insolation. Transmittance values clearly differ according to the atmospheric conditions. The difference between the maximum and the minimum values at each solar zenith angle is found to be about 15 % throughout the range. A large monthly variation of clear-sky transmittance is also found, especially for April. It is consistent with the fact that the surface flux is more sensitive to the water vapor amount when it becomes drier, as indicated in Fig. 1 of Chou and Zhao (1997). This large monthly variation of clear-sky transmittance proves how difficult it is to obtain the clear-sky flux purely from the surface flux observations.

Figure 4 depicts the time series of the daily-mean clear-sky transmittance for the total (direct+diffuse) shortwave flux as well as its direct-flux component for 1996. An annual variation is found

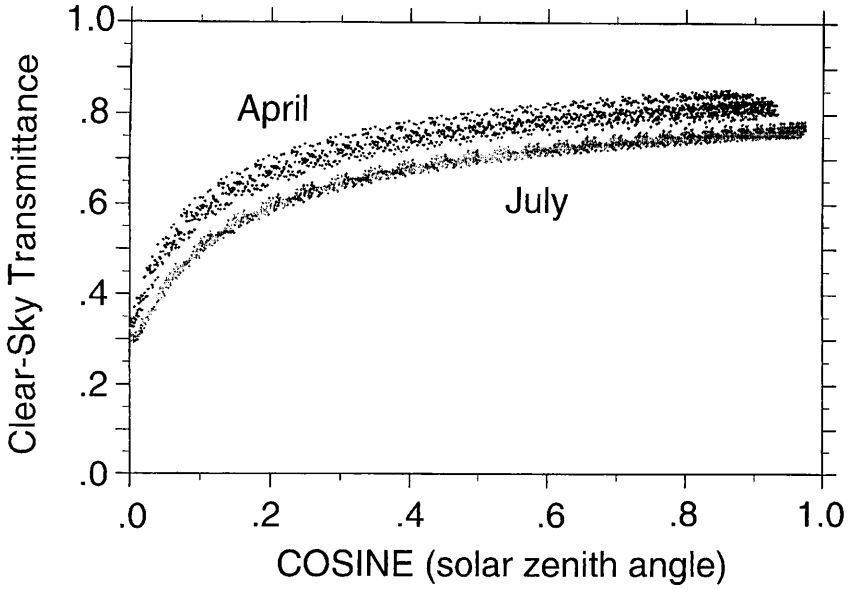

Fig. 3. Clear-sky shortwave transmittance (surface downward flux/TOA insolation) plotted versus the cosine of the solar zenith angle, for April (upper group of darker dots) and July (lower group of lighter dots) 1996.

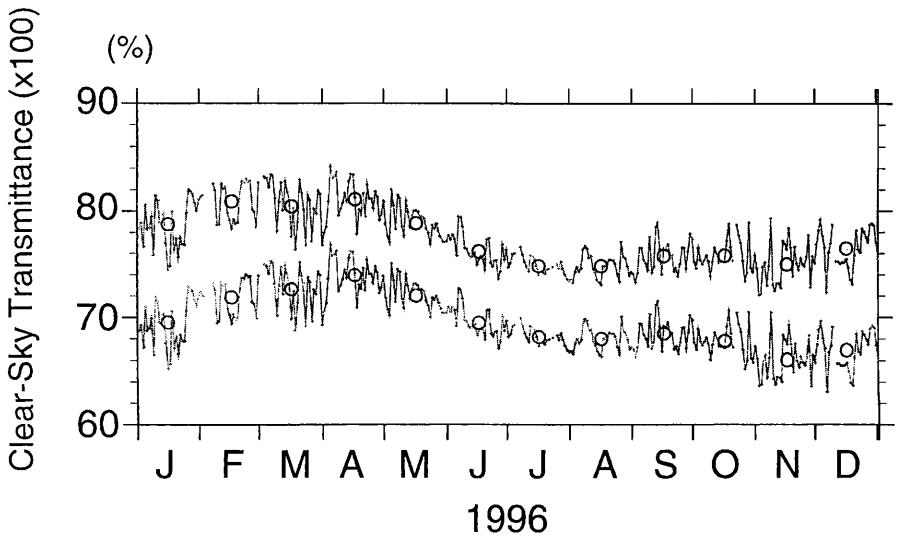

Fig. 4. Time series of the calculated clear-sky total surface shortwave flux (upper curve) and the direct component (lower curve) in percent fraction relative to the TOA solar insolation for 1996. Daily averages are depicted with small dots connected with lines and open circles indicate the monthly averages.

with relatively transparent atmosphere in the earlier half of the year, and with larger absorption in the latter. Relatively larger day-to-day variations are found in the cooler months, from October to April, when the atmosphere is relatively drier.

Table 1 shows the monthly-mean values related to the clear-sky transmittance. The maximum monthly-mean transmittance is found in February and April. The minimum value is found in August. As seen in Fig. 3, the clear-sky transmittance is a function of the solar zenith angle as well as a function of the water vapor loading. Transmittance is higher for the smaller solar zenith angle. It is considered that the maximum transmittance in February results from the minimum column water vapor amount (CWVP), while that in April results from a low CWVP with a moderate mean solar zenith angle. Although the solar zenith angle is small, abundant water vapor in the atmosphere is lowering the clear-sky transmittance in the summer months.

5. Aerosol-sky flux calculations

Aerosol optical depths retrieved from the sky radiometer measurements were adopted for the

Table 1. Monthly mean values for the insolation ($F0$) and clear-sky surface downward shortwave flux (F_{clear}) in W m^{-2}; transmittance ($F_{clear}/F0$); atmospheric column water vapor amount in kg m^{-2} ($CWVP$); and the cosine of the solar zenith angle ($cosz$). $F0$ and F_{clear} values are based on the daily average for the days when the flux observations are available.

month	$F0$	F_{clear}	$F_{clear}/F0$	$CWVP$	$cosz$
JAN	187.	148.	.791	7.7	.300
FEB	217.	176.	.811	7.6	.377
MAR	335.	269.	.803	12.1	.497
APR	407.	330.	.811	11.8	.623
MAY	454.	358.	.789	21.7	.710
JUN	472.	359.	.761	39.5	.754
JUL	458.	343.	.749	47.4	.759
AUG	421.	315.	.748	44.3	.728
SEP	358.	271.	.757	32.1	.652
OCT	279.	212.	.760	23.4	.539
NOV	206.	156.	.757	19.7	.408
DEC	183.	140.	.765	10.1	.314

aerosol-sky flux calculations. In Figs. 5(a) and (b), examples of calculated aerosol-sky fluxes (large dots), and the observed values (small dots), are depicted for the afternoon observations of 19 June and for those of 19 May 1996, respectively. The DRC and DF in Fig. 5 stand for the direct and diffuse components, respectively. Clear-sky flux (crosses) and TOA flux values (straight line) are also shown. Here, for the first experiments, the chemical composition and the size distribution were adopted from the model urban (soot weight fraction of 20 %) atmosphere in LOWTRAN 7.

The afternoon of 19 June 1996 was extremely clear for this season of the year. The daily-mean aerosol optical depth was as small as 0.13. In the afternoon of 19 May 1996, the atmosphere was relatively polluted with a daily-mean aerosol optical depth of 0.52. By comparing the calculations with observations, the discrepancy is very small for the case of 19 June, with -0.5 W m^{-2} for direct component, and -0.2 W m^{-2} for diffuse flux component for a daily-mean-equivalent. For the case of 19 May, the discrepancies have considerable values of -12.9 W m^{-2} for direct, and -6.1 W m^{-2} for diffuse flux in the same manner.

As described in Section 2, the aerosol forcing is defined by the difference between the calculated flux (positive downward) for the aerosol-sky and that for the clear-sky. It is seen from the figures that the instantaneous aerosol forcing amount is around -50 W m^{-2} for the direct flux and around $+20$ W m^{-2} for the diffuse flux for the case of 19 June. As for the case of 19 May, the direct flux forcing reaches almost -300 W m^{-2}, while the diffuse flux compensates it by around $+150$ W m^{-2}.

For the above calculations, we adopted the urban-model aerosol chemical composition and size distributions from LOWTRAN 7. However, the calculated flux values are sensitive to the assumed aerosol optical properties, especially to the refractive index. Soot affects the imaginary part of the refractive index most efficiently. In order to estimate the aerosol and cloud radiative forcing to the surface radiation accurately, it is indispensable to determine the weight fraction of soot in aerosols appropriately.

We examined the sensitivity of the aerosol-sky flux calculations to the soot weight fraction. We performed the aerosol-sky flux calculations with the soot fraction of 20, 10, 5, and 0 %. The aerosol composition for soot fraction of 20 % case was chosen as identical to the model urban atmosphere of LOWTRAN 7, with 56 % water soluble and 24 % dust-like aerosols. That for soot fraction of 0 % was chosen as identical to the model rural atmosphere with 70 % water soluble and 30 % dust-like. Other cases were in linear relations with these two. Real parts of refractive indices are 1.52–1.53, 1.52–1.53, and 1.75; and imaginary parts are 0.005–0.017, 0.008, and 0.43–0.47; for water soluble, dust-like, and soot, respectively, for the wavelength range of sky radiometer channels.

Figures 6(a) and (b) show the monthly mean calculation errors (Aerror) of daily-mean-equivalent aerosol-sky shortwave flux for the sensitivity experiments. Figure 6(a) is for the diffuse flux normal to the horizontal surface, and (b) is for the direct flux. It is obvious that for the soot weight fraction of 20 % (urban aerosol), the diffuse flux significantly underestimates for the warmer months from May through September, while the error is very small from October through December. The sensitivity of the diffuse flux to the soot variation of 0–20 % range varies from 40 W m^{-2} for May to 8 W m^{-2} for January.

Among the selected soot fraction, the best estimates regarding the diffuse flux are the soot fractions of 10 % for January and July, 20 % for February and October through December, 5 % for May, June and August, and 0 % for September. These estimates are nearly consistent with the measurements by Ohta and Okita (1984), which reported the weight fraction of the elemental carbon to the total suspended particulates (EC/TSP) in Sapporo varying between 0.09 in April and 0.23 in February, and the ratio of the elemental carbon to total suspended particulates excluding seasalt (EC/NSS TSP) along the Pacific coast of Japan from Kawasaki to Hyuga. This was almost uniform with the value of about 0.1.

As for the direct flux, the error is not very sensitive to the soot ratio as shown in Fig. 6(b). How-

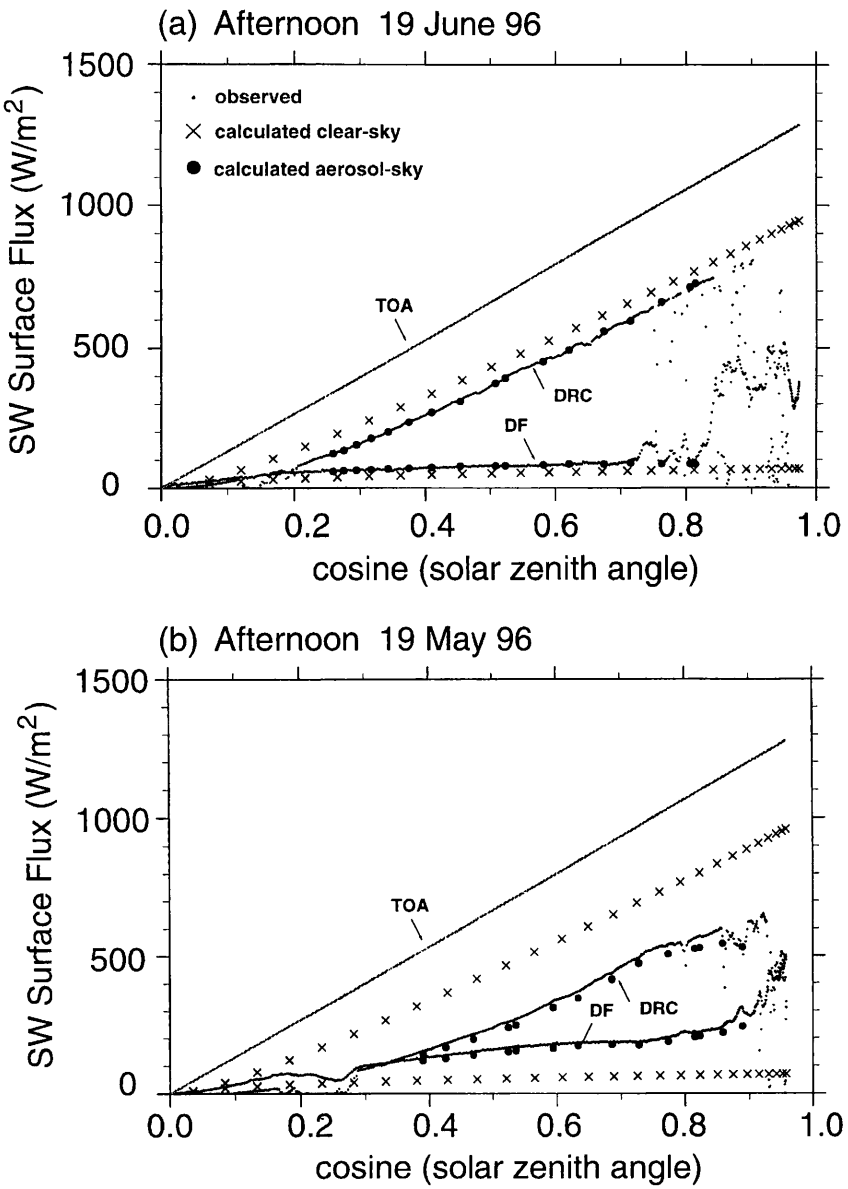

Fig. 5. Direct and diffuse parts of solar flux from 1-min.–averaged pyrheliometer and pyranometer measurements (small dots), from clear-atmosphere calculations (crosses), and from aerosol-laden-atmosphere calculations (large dots) for (a) the afternoon of 19 June and for (b) the afternooon of 19 May, 1996 plotted against the cosine of the solar zenith angle. DRC and DF indicate the direct and diffuse components, respectively. Straight line depicts the shortwave insolation at the top of the atmosphere (TOA). Mean aerosol optical thickness for the light wavelength of 5 μm was 0.13 for (a) and 0.52 for (b).

ever, it is noticed that for some months, January, February and July, the error values are greater than 10 $W m^{-2}$. A candidate for causing the large error in the direct flux calculation may be the adopted size distributions. By using the retrieved size distribution from the sky radiometer measurements, the direct flux underestimates even significantly, by as large as 40 $W m^{-2}$ especially for May, June and July for the case with soot fraction of 20 % (not shown here). The error is found to be largest for June and smallest for January.

Therefore, we next compared the retrieved size distributions with the urban model size distribution (Fig. 7). The upper panel shows the volume distribution of aerosols, while the lower panel shows the surface area distribution. Note that the refractive index of 1.5–0.01i was assumed for the retrieval. It was shown in Shiobara *et al.* (1991) that the refractive index does not greatly affect the retrieval of the size distributions. For the case of June, when the direct flux error for the estimates with the retrieved size distributions was large, it is found that the

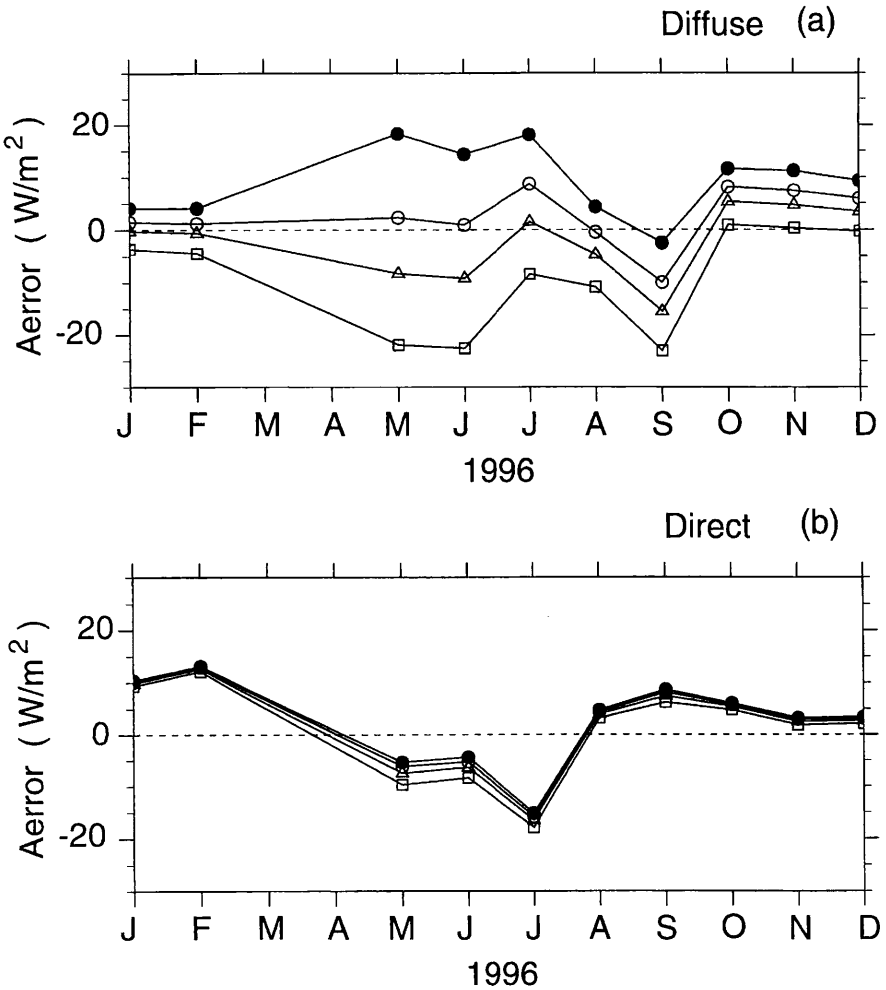

Fig. 6. Monthly mean daily-mean-equivalent errors of aerosol-sky flux calculated with soot weight fraction of 20, 10, 5, and 0 %, which are marked with squares, triangles, open circles and closed circles, respectively. The abscissa is the month and the ordinate is the difference between the calculated and observed values of the global downward shortwave flux, for (a) the diffuse component, and for (b) the direct component.

retrieved aerosol concentrations are overestimated over all the size range. Considering that the total surface area of particles determines the shortwave scattering and absorption, the overestimate of finer particles seems to almost affect the same amount with that of giant particles, assuming the urban model distribution was realistic (Fig. 7(b)). For January, on the other hand, the calculated flux with the retrieved size distribution agrees better with the observation than that with the urban-model size distribution. In this case, smaller particles are estimated to be even less than the urban model. Error values larger than 10 W m^{-2} in the direct flux were found from May to September (not shown), which coincide with the period when the water vapor column amount is large. It might be that some unrealistic size distributions were retrieved in relation to such atmospheric conditions. Further examinations on the retrieval of the aerosol size distribution using the sky radiometer measurements are necessary.

Relatively large errors in the direct flux estimates may also be caused by an inappropriate assumption on the chemical compositions in retrieving the aerosol optical depths from the sky radiometer data. Therefore, we used the optical depth values retrieved from the sun photometer-type algorithm, which does not depend on the aerosol chemical compositions, and performed the same sensitivity study. Figure 8 shows that for the same error estimates, but utilizing the optical depths retrieved from the sun photometer-type method. From Fig. 8(b), it is noticed that direct flux estimates are mostly improved within the error of about 10 W m^{-2} except for the period from August to October. As for the best estimates of soot fraction, they coincided mostly with the first experiment but with changes from 10 % to 20 % for January and February. As a result, the soot fraction estimates were not very sensitive to the

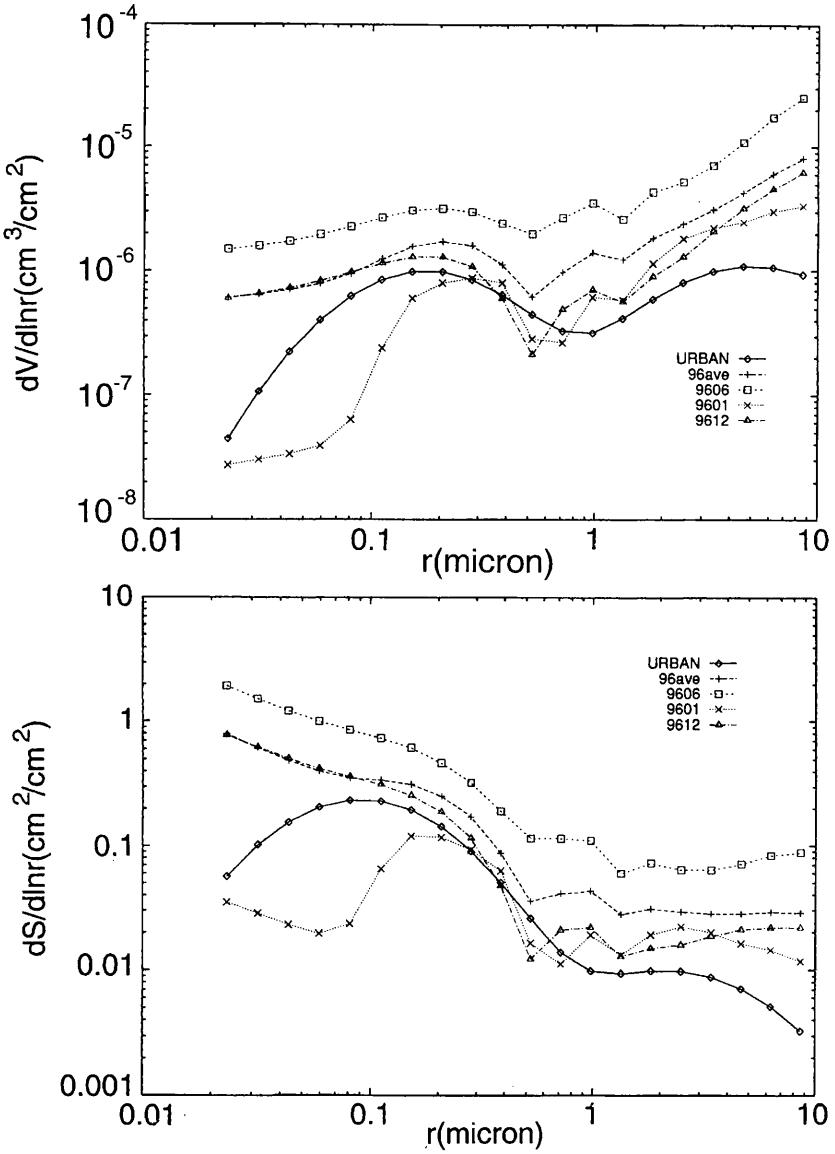

Fig. 7. Aerosol size distribution retrieved from the skyradiometer measurements for January, June, December, and a yearly-mean of 1996 compared with that of the LOWTRAN 7 urban model. The upper panel shows the volume distribution in cm^3/cm^2 and the lower panel shows the surface area distribution in cm^2/cm^2 versus the radius in μm.

retrieval method of the optical thickness, although the sun photometer-type method seems to perform a little better from the point of the direct flux estimates. Hereafter, we adopt the values calculated with the original optical depths, since it provides us with more numbers of available data.

Referring to the yearly-average NO_2 concentrations cited from *the Annual Report on Ambient Air-Pollution Monitoring at General Stations*, the third quadrant (open to southwest) area relative to Tateno is quite polluted, while to the north of Tateno is relatively rural. Considering such locations, the results of the above sensitivity tests were consistent with the lower-level wind directions obtained from the upper atmospheric observations (not shown here). From May to July as well as from October to December, winds from the third urban quadrant were dominant. For January and February, the wind was from the second quadrant where the urbanization was intermediate. Larger soot fraction suggested for January and February compared to the warmer season was probably due to larger combustion during the wintertime. From October through December, local biomass burning after the rice harvest may be putting additional soot to the transported urban air. For September with a good fit with the case with the soot fraction of 0 %, the easterly wind from rural area was dominant. September 1996 indeed was a clear month, however, the soot fraction of 0 % may be too small

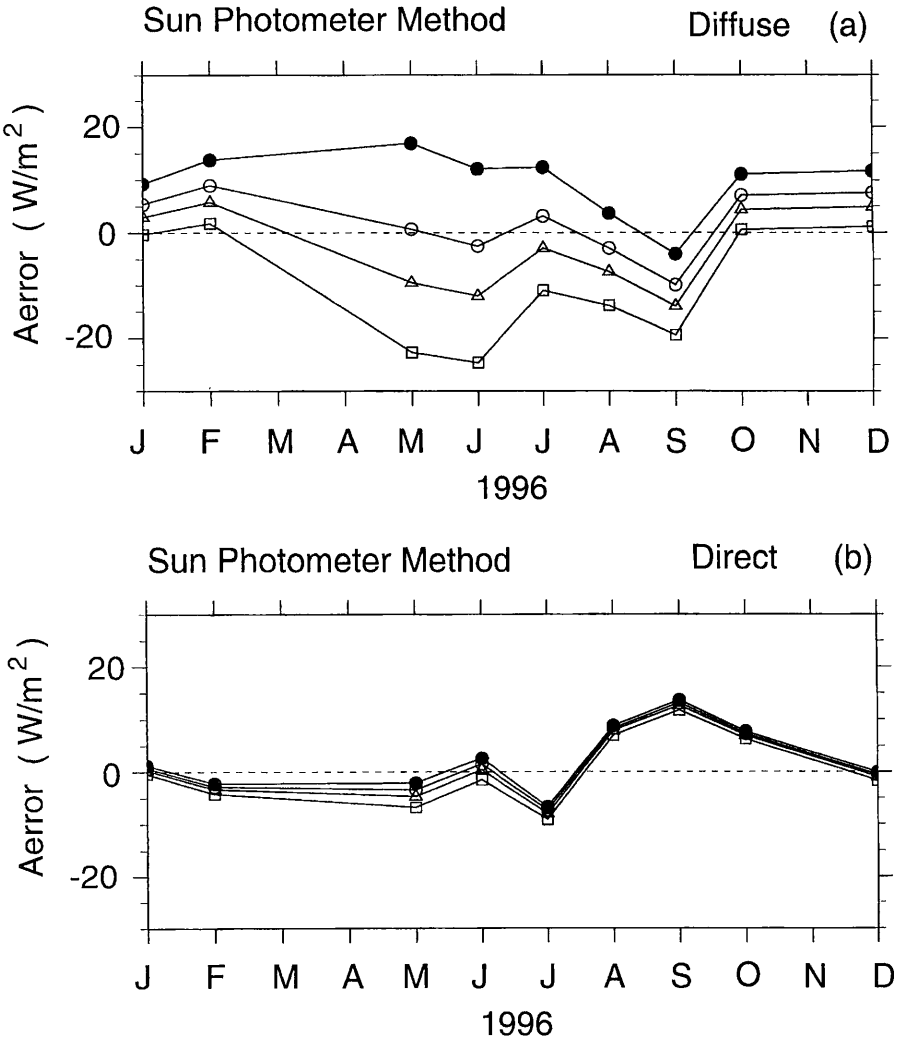

Fig. 8. Same as Fig. 6 but calculated with aerosol optical depths retrieved with sunphotometer-type method.

for any observation in a suburban town. This result suggests that some errors reside in the retrieved aerosol properties. Further examinations on their retrieval methods are necessary for future studies.

6. Estimate of the cloud and/or aerosol radiative forcing at the surface

Finally, the daily cloud+aerosol forcing (CAF) values and the daily aerosol forcing (AF) values obtained for the entire analysis period are depicted in Fig. 9. For this annual aerosol forcing calculation, best estimates of soot ratio regarding the diffuse flux for each month were selected: 10 % for January and July, 20 % from February and October through December, 5 % for May, June and August, and 0 % for September. Note that the assumption of soot fraction influences AF values, but does not affect the CAF amounts.

Annual march of the CAF amounts roughly follows the variation of the insolation, but also reflects the seasonality of the cloud amount. The annual mean values are -81 W m^{-2} for CAF, and -18 W m^{-2} for AF (Table 2). These values correspond to about 24 % and about 6 % of the insolation, respectively.

Errors accompanying the above estimates are also shown in Table 2. The annual mean error of the daily-mean-equivalent aerosol-sky flux is 3.6 W m^{-2} for direct flux, and 0.0 W m^{-2} for diffuse flux. The rms errors are 22.4 W m^{-2} for direct and 19.7 W m^{-2} for diffuse flux (not shown here). For a reference, in the ninth and the tenth columns, daily-mean-equivalent errors for calculations with the aerosol optical depths using the sun photometer-type method described in the former section are also shown. The annual-mean direct flux error reduces to -1.3 W m^{-2} while that for the diffuse flux slightly increases to 0.9 W m^{-2}.

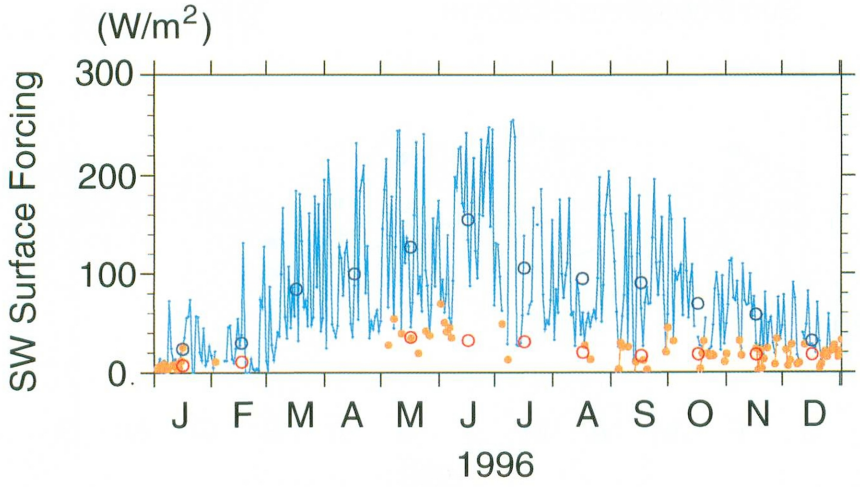

Fig. 9. Time series of the cloud+aerosol, and aerosol solar radiative forcing at Tateno for 1996 depicted in W m^{-2}. Daily means are depicted with dots connected with lines and monthly means are depicted with open circles. Those in bluish colors are for CAF, and in reddish colors are for AF.

Table 2. Monthly means of TOA insolation ($F0$), surface cloud+aerosol shortwave forcing (CAF), surface aerosol forcing (AF), and daily-mean-equivalent errors of aerosol-sky flux calculations for the direct component of the downward flux (AE_{DRC}) and diffuse component (AE_{DF}), respectively, in W m^{-2}. N_{day} and N_{obs} indicate the numbers of days and observations included in the statistics of the aerosol-sky flux. Daily-mean-equivalent errors for calculations with the aerosol optical depths using the sunphotometer-type method are also shown in the ninth and the tenth columns for the direct component (AE^{SP}_{DRC}) and diffuse component (AE^{SP}_{DF}), respectively, in W m^{-2}.

month	$F0$	CAF	AF	AE_{DRC}	AE_{DF}	N_{day}	N_{obs}	AE^{SP}_{DRC}	AE^{SP}_{DF}
JAN	201.1	−24.4	−7.8	9.9	−0.2	21	517	0.4	0.3
FEB	249.7	−34.9	−9.0	12.6	−0.6	3	89	4.2	−1.8
MAR	334.6	−84.5	—	—	—	0	0	—	—
APR	407.3	−99.9	—	—	—	0	0	—	—
MAY	453.5	−127.0	−35.1	−6.2	2.3	9	196	3.4	−0.7
JUN	471.6	−154.8	−31.9	−5.3	0.9	5	114	−1.5	2.5
JUL	458.2	−96.5	−30.6	−16.5	1.5	2	40	8.0	2.9
AUG	420.9	−95.0	−19.9	4.4	−0.5	2	92	−8.3	2.9
SEP	358.1	−90.6	−16.4	8.7	−2.5	10	214	−13.6	4.0
OCT	290.6	−69.8	−18.0	4.8	0.9	10	271	−6.3	−0.6
NOV	218.5	−60.4	−17.6	1.8	0.3	10	217	—	—
DEC	183.6	−31.7	−17.6	2.1	−0.3	19	485	1.7	−1.2
YRave	337.5	−80.8	−17.8	3.6	0.0	91	2235	−1.3	0.9

7. Discussion and summary

In this study, we integrated pyrheliometer and pyranometer radiative flux measurements, radio-sonde atmospheric profile measurements, the sky radiometer measurements of aerosols, and a high accuracy state-of-the-art transfer model calculations. The cloud+aerosol shortwave radiative forcing and the aerosol forcing have been estimated at the surface for a year of 1996 at Tateno.

Clear-sky flux was defined from transfer calculations for a Rayleigh-scattering atmosphere utilizing the measured temperature and humidity profiles from radio-sonde observations. This method had two distinct advantages. First, it enabled us to treat the aerosol effect separately from the Rayleigh-scattering molecules. Second, we could then obtain the clear-sky flux simultaneously with the total-sky flux measurements, with explicitly prescribed atmospheric profiles. Monthly variation of the clear-sky flux due to the temperature and the water vapor was found to be 10–30 W m^{-2} at Tateno.

We defined the cloud+aerosol forcing by differentiating the observed flux and the above clear-sky flux. Then, aerosol forcing was obtained from the difference between the aerosol-sky flux and the clear-sky flux. We also obtained the error estimates for the aerosol-sky flux by comparing the observed

flux, and the calculated aerosol-sky flux for the clear days. The surface flux calculations with the retrieved aerosol size distributions performed no better than those with the urban-model size distribution. It was attributed to the overestimate of the fine particles as well as the giant particles.

We also examined the dependency of the aerosol-sky flux estimates on the aerosol optical properties, especially by varying the fraction of the soot component. It was suggested that Tateno is characterized as a suburban town with aerosol properties corresponding between that of the model urban aerosols (soot weight fraction of 20 %) and the model rural aerosols (soot weight fraction of 0 %). Seasonalities of the combustion as well as of the winds are probably affecting the aerosol chemical properties at this site. The assumption for the aerosol chemical composions at the stage of retrieving the aerosol optical depths from the sky radiometer data may influence the results. Therefore, we additionally performed the same sensitivity study using the optical depths retrieved with the sun photometer-type method. Errors for direct flux calculations were improved, although the results were not very much changed.

Finally, the annual mean value of the cloud +aerosol surface shortwave forcing was estimated as $-81\ \mathrm{W\,m^{-2}}$. The mean aerosol forcing for 1996, but for March and April, was estimated as $-18\ \mathrm{W\,m^{-2}}$. These values correspond to about 24 % and about 6 % of the insolation, respectively.

Not to mention the indirect aerosol forcing, there are remaining problems for further studies. There are uncertainties resulting from the assumptions on aerosol chemical compositions, size distributions, and vertical distributions. The uncertainties in upper-level water vapor observations cannot be ignored. It is also necessary to remember that we are missing the aerosol data for March and April when we expect frequent Kosa events. However, few precedent studies were found for the precise statistical estimates of the cloud and/or aerosol shortwave forcing. Therefore, even with certain amounts of assumptions, we think we could present a new quantitative aspect of the surface cloud and/or aerosol shortwave forcing amounts , as well as we could show the effectiveness of the closure of various measurements for the radiative forcing calculations.

Acknowledgments

A part of this research was supported by the Japanese Ministry of Education, Science, Sports and Culture under Grant-in-Aid for Scientific Research on Priority Areas No. 09227224.

One of the authors is indebted to Dr. Akiko Higurashi at NIES and Mr. Takashi Nakajima at NASDA for their help and suggestions in utilizing the transfer calculation package RSTAR5. Drs. Miwako Ikegami, Yuji Zaizen at MRI, Dr. Tsutomu Fukuyama at NIES, and Prof. Sachio Ohta in Hokkaido University also provided her with knowledge of the observed aerosols. She expresses her sincere thanks to them. Helpful comments from Dr. Kikuo Okada and anonymous reviewers are gratefully acknowledged.

References

Arking, A., 1996: Absorption of solar energy in the atmosphere: Discrepancy between model and observations. *Science*, **273**, 779–782.

Cess, R.D., 1995: Absorption of solar radiation by clouds: observations versus models. *Science*, **267**, 496–499.

Charlson, R.J., S.E. Schwartz, J.M. Hales, R.D. Cess, J.A. Coakley Jr., J.E. Hansen and D.J. Hofmann, 1992: Climate forcing by anthropogenic aerosols. *Science*, **255**, 423–430.

Chou, M.-D. and W. Zhao, 1997: Estimation and model validation of surface solar radiation and cloud radiative forcing using TOGA COARE measurements. *J. Climate*, **10**, 610–620.

Conant, W.C., V. Ramanathan and F.P.J. Valero, 1997: An examination of the clear-sky solar absorption over the central equatorial Pacific: Observations versus models. *J. Climate*, **10**, 1874–1884.

Hayasaka, T., N. Kikuchi and M. Tanaka, 1995: Absorption of solar radiation by stratocumulus clouds: Aircraft measurements and theoretical calculations. *J. Appl. Meteor.*, **34**, 1047–1055.

Haywood, J.M. and K.P. Shine, 1995: The effect of anthropogenic sulfate and soot aerosol on the clear sky planetary radiation budget. *Geophys. Res. Lett.*, **22**, 603–606.

Kiehl and Briegleb, 1995: The relative roles of sulfate aerosols and greenhouse gases in climate forcing. *Science*, **260**, 311–314.

Kneizys, F.X., E.P. Shettle, L.W. Abreu, J.H. Chetwynd, G.P. Anderson, W.O. Gallery, J.E.A. Selby and S.A. Clough, 1986: Users guide to LOWTRAN 7, Rep. *AFGL-TR-88-0177*, Air Force Geophys. Lab., Hanscom AFB, Mass.

Nakajima, T. and T. Hayasaka, A. Higurashi, G. Hashida, N. Moharram-Nejad, Y. Najafi and H. Valavi, 1996: Aerosol optical properties of Persian Gulf reation Part I. Gound-based solar radiation measurements in Iran. *J. Appl. Meteor.*, **35**, 1265–1278.

Nakajima, T. and M. Tanaka, 1983: Effect of wind-generated waves on the transfer of solar radiation in the atmosphere-ocean system. *J. Quant. Spectrosc. Radiat. Transfer*, **29**, 521–537.

Nakajima, T. and M. Tanaka, 1986: Matrix formulations for the transfer of solar radiation in a plane-parallel scattering atmoshere. *J. Quant. Spectrosc. Radiat. Transfer*, **35**, 13–21.

Nakajima, T. and M. Tanaka, 1988: Algorithms for radiative intensity calculations in moderately thick atmospheres using a truncation approximation. *J. Quant. Spectrosc. Radiat. Transfer*, **40**, 51–69.

Ohta, S. and T. Okita, 1984: Measurements of particulate carbon in urban and marine air in Japanese areas. *Atmos. Environ.*, **18**, 2439–2445.

Pilinis, C., S.N. Pandis and J.H. Seinfeld, 1995: Sensitivity of direct climate forcing by atmospheric aerosols to aerosol size and composition. *J. Geophys. Res.*, **100**, 18739–18754.

Pilewskie, P. and F.P.J. Valero, 1995: Direct observations of excess solar absorption by clouds. *Science*, **267**, 1626–1629.

Ramanathan, V., G. Subasilar, G.J. Zhang, W. Conant, R.D. Cess,J.T. Kiehl, H. Grassl and L. Shi, 1995: Warm pool heat budget and shortwave cloud forcing: A missing physics? *Science*, **267**, 499–503.

Shiobara, M., T. Hayasaka and M. Tanaka, 1991: Aerosol monitoring using a scanning spectral radiometer in Sendai, Japan. *J. Meteor. Soc. Japan*, **69**, 57–70.

Stephens, G.L., 1996: How much solar radiation do clouds absorb? *Science*, **271**, 1131–1133.

Wild, M., A. Ohmura and H. Gilgen, 1995: Validation of general circulation model radiative fluxes using surface observations. *J. Climate*, **8**, 1309–1324.

観測と放射伝達計算による地表面放射への雲とエアロゾルの影響の見積 Part I：館野における短波放射強制力

高薮 縁
（国立環境研究所）
上野丈夫
（気象庁高層気象台）
中島映至
（東京大学気候システム研究センター）
松井一郎
（国立環境研究所）
對馬洋子
（東京大学気候システム研究センター）
青木一真
（北海道大学）
杉本伸夫
（国立環境研究所）
鵜野伊津志
（九州大学）

雲とエアロゾルの地表面短波放射強制力の年間値を見積もるために、館野における精度のよい短波放射観測値、ラジオゾンデ観測値およびスカイラジオメター観測によるエアロゾルの光学的特性値を用いて高精度放射伝達計算を行なった。

晴天フラックスは、ラジオゾンデ観測による温度湿度プロファイルを用いた純粋なレイリー散乱大気についての計算により定義した。水蒸気と温度プロファイルによる晴天フラックスの月変化は 10–30 $\mathrm{W\,m^{-2}}$ であった。雲とエアロゾルによる地表面短波放射強制力はフラックス観測値と晴天フラックスとの差によって定義した。1996 年の年間平均値は $-81\ \mathrm{W\,m^{-2}}$ であり、大気上端の太陽入射の約 24 %に当たる。一方、エアロゾル強制は、スカイラジオメター観測によるエアロゾルの光学的厚さを用いた大気フラックスの計算値と晴天フラックスとの差によって求めた。3–4 月を除く年間平均値は $-18\ \mathrm{W\,m^{-2}}$ で、6 %にあたる。

エアロゾルに含まれる煤の割合に対する感度実験の結果、1 月、2 月、7 月は 10 %、10–12 月は 20 %、5 月、6 月、8 月は 5 %、9 月は 0 %の煤の割合が推定された。この値は、これまでに観測されている煤の割合や都市分布と風向の関係と概ね一致する。

ただし、スカイラジオメターから求めたエアロゾルの粒径分布を計算に用いると、特に大気水蒸気量の多い夏期において推定値の誤差が拡大した。スカイラジオメター観測データを用いたエアロゾル粒径分布の推定手法について、今後の詳細な検討の必要性が示唆される。